CHAPTER 6

INVESTIGATION ON THE 4-ELEMENT COMPOSITE TRIANGULAR DIELECTRIC RESONATOR ANTENNA USING LMAP CERAMIC

6.1 Introduction

In recent times, dielectric resonator antennas (DRAs) attracted the attention of researchers due to their remarkable properties, such as large bandwidth, high radiation efficiency, high gain, low loss, compatibility with different excitation techniques and less spurious feed radiation [Petosa (2007)]. Many shapes such as rectangular, cylindrical, cubic, cylindrical ring, spherical, hemispherical, chamfered, conical, elliptical, tetrahedral, filleted and triangular geometries have been widely investigated [Luk and Leung (2003); Sharma and Gangwar (2017b); Guha et al. (2015a); Kumar and Chaudhary (2016); Mongia et al. (1993b); Ittipiboon et al. (1993); Haneishi and Takazawa (1985); Kishk et al. (2002, 2003a, 2003b); Tripathi et al. (2018)]. The DRA with triangular geometry is more compact in size when compared with rectangular and cylindrical shaped DRAs [Gangwar et al. (2017)].

Different shapes and composite structures have been investigated for DRAs with broadside radiation. But only handful of investigations are available in literature for providing monopole type radiation pattern. Coaxial fed dielectric ring resonator with TM_{01} mode was used to generate monopole like radiation [Mongia et al. (1993b)]. An electric monopole fed dielectric ring has been reported as an ultra-wideband antenna [Lapierre et al. (2005)]. Four element cylindrical [Guha et al. (2006)], rectangular [Rajan and Gangwar (2013)] and triangular [Gangwar et al. (2017)] DRAs have been reported

for obtaining monopole like radiation pattern. Enhanced bandwidth is the major design consideration for DRAs. Various bandwidth enhancement techniques have been discussed in literature, such as the use of low dielectric constant materials, stacking of DRAs with different dielectric constants, introducing notch/air gap between DRA element and ground plane using different feeding techniques, sectoring and splitting of the DRA elements etc. [Mongia et al. (1993a, 1993b); Shum and Luk (1994); Junker et al. (1994a, 1994b); Ittipiboon et al. (1996); Tam and Murch (1998)].

The material selection plays an important role in the design and development of DRAs. Generally, materials with good microwave dielectric properties i.e. those having low loss and dielectric constant (ε_r) values in the range 5 – 50 [Zou et al. (2017)] have found wide application in the design of DRAs. The Lithium magnesium phosphate based ceramics possess good microwave dielectric properties. The Li_2O–1.94MgO–0.02Al_2O_3–P_2O_5 (LMAP) ceramic having dielectric constant ε_r = 6.2 and tanδ = 0.0006 was used as low temperature co-fired ceramic (LTCC) substrate application for design and development of the Dual Segment Cylindrical DRA [described in Chapter 5]. The LMAP ceramic is also a viable material for resonating element for the design of antenna.

In the present chapter, four element composite triangular DRA (4–CTDRA) with each triangular element consisting of a combination of the LMAP ceramic (ε_r = 6.2 and tanδ = 0.0006) and teflon (ε_r = 2.1 and tanδ = 0.0010) sections has been investigated through simulation and performance study of the prototype antenna fabricated in the laboratory. A parametric study through simulation using Ansys High Frequency Structure Simulator (HFSS) software was performed by varying the structural parameters i.e. side lengths of the composite DRA elements, dielectric constant of the composite elements, and probe height on the input reflection coefficient – frequency characteristic. In proposed 4–

CTDRA, TM^{z}_{101} mode is excited in each DRA element. The simulated near field distribution for TM^{z}_{101} mode results in monopole like radiation pattern over wide bandwidth. Input and radiation characteristics are compared with experimental results. Further, radiation characteristics of the proposed antenna are also compared with similar work reported in literature [Gangwar et al. (2017); Guha et al. (2006); Chaudhary et al. (2012)]. The proposed antenna provides wide impedance bandwidth (61.65 % (simulated) and 66.09 % (measured)) with monopole like radiation pattern.

6.2 Material description

Li_2O–1.94MgO–0.02Al_2O_3–P_2O_5 (LMAP) was synthesized by conventional solid state route as described in Chapter 3. The ceramic samples with triangular geometry (each side length = 4 mm and height = 11 mm) were prepared and sintered at 825 ^{o}C for 6 h with heating and cooling rate of 2 ^{o}C per minute. The ceramic is found to possess average dielectric constant value of 6.2 and loss tangent of 0.0006 within the entire frequency range. Another material, Teflon is also shaped in trapezoidal geometry as per the dimension given in Table 6.1.

6.3 Antenna design and fabrication

Figure 6.1 shows geometrical representation of the proposed TDRA. The antenna design parameters are illustrated in Table 6.1. The complete TDRA is placed on square ground plane of copper of size 60 mm × 60 mm × 0.5 mm. From practical point of view, it is easier to excite the triangular DRA elements directly with coaxial probe from one of their corners than using modified probe for exciting CDRA [Guha et al. (2006)] and RDRA [Rajan and Gangwar (2013)] elements. The proposed antenna geometry meets the requirements of bandwidth enhancement through introduction of low dielectric constant

material (air) around the elements and the use of high dielectric constant material (LMAP) touching the probe. Though the proposed antenna consists of more number of dielectric blocks as compared with previous designs [Guha et al. (2006); Rajan and Gangwar (2013); Gangwar et al. (2017)], it shows some added advantages, such as simpler design and easier optimization of parameters, planar geometry with compact size and improved bandwidth. Some studies on multi–element DRAs using composite feed structure [Guha et al. (2006)] and multi–layer multi–permittivity composite feed structure [Chaudhary et al. (2012)] increases the fabrication complexity. In this chapter, emphasis has been given on the development of DRA to provide wideband monopole like radiation pattern with ease of fabrication. The RADIALL make 3.5 mm SMA (sub-miniature version A) connector with optimized probe height of 5.7 mm above the ground plane is centrally fixed on the ground plane for excitation of the proposed DRA. Four composite dielectric blocks are placed on metallic ground plane having uniform spacing of 30^{o} touch a portion (5.7 mm) of a corner of each block. Each composite dielectric block consists of two sections: one section contacting the probe which is of triangular cross-section is made of LMAP with $\varepsilon_r = 6.2$ and $\tan\delta = 0.0006$, and the second section, which doesn't touch the probe has trapezoidal geometry and is made of teflon with $\varepsilon_r = 2.1$ and $\tan\delta = 0.0010$. The fabricated antenna is shown in Figure 6.2.

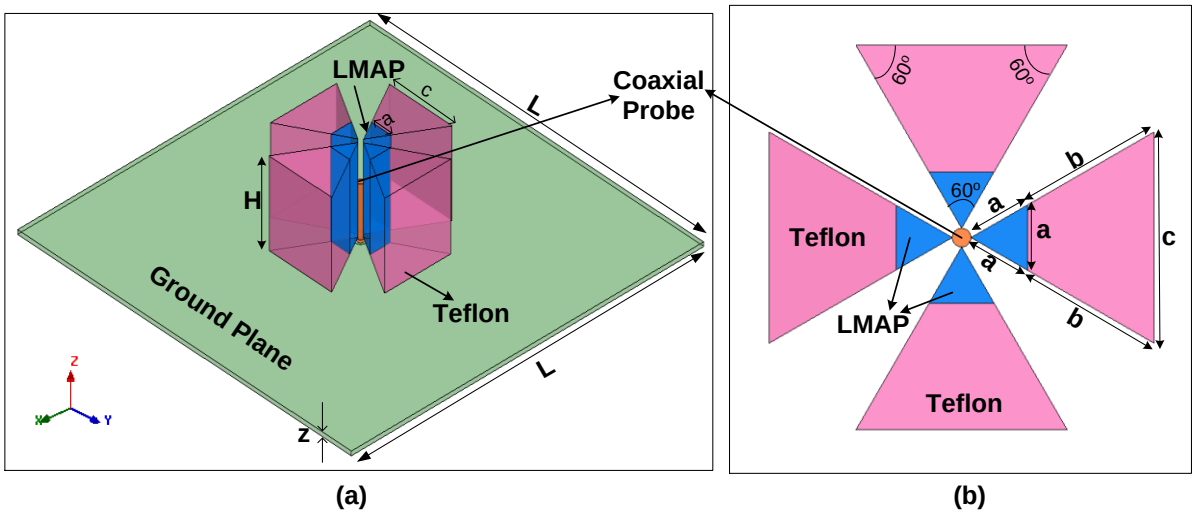

Figure 6.1 Geometry of proposed composite TDRA (a) 3D view and (b) Top view.

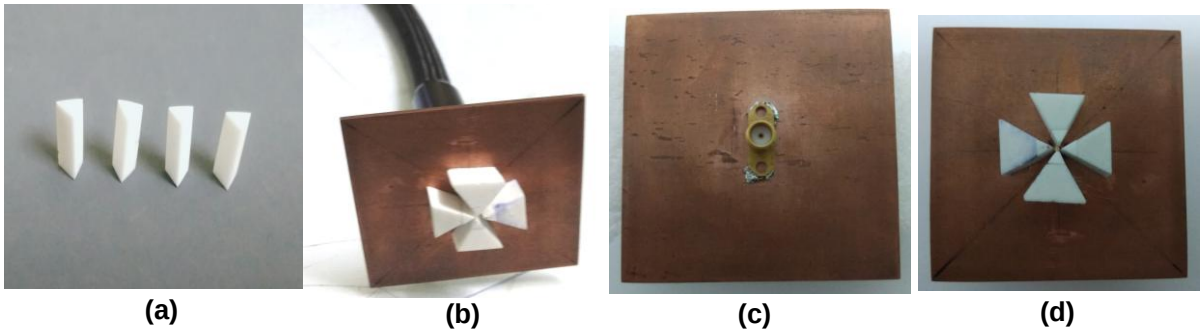

Figure 6.2 Image of the fabricated composite TDRA (a) Triangular ceramic components, (b) 3D view, (c) Bottom side and (d) front side.

Table 6.1 Antenna design parameters

Optimized Parameters	**Dimensions**
Substrate dimension, $L \times L \times z$	60 mm × 60 mm × 0.5mm
Height of each triangular element, H	10 mm
Side length, a	3.464 mm
Side length, b	7.794 mm
Side length, c	11.258 mm
Probe height above the ground plane, H_p	5.7 mm
Probe radius, R_p	0.5 mm
Internal angle of triangle	60^o

The input characteristics of the proposed antenna was measured using Keysight make Network Analyser (Model E5071C) and its radiation characteristics was measured inside the fully automated anechoic chamber (shown in Figure 6.3). The fabricated prototype of the antenna (antenna under test (AUT)) was fixed on the top of the rotating table, as shown in Figure 6.3(b). A TEM horn antenna (shown in Figure 6.3(a)) is used as transmitting antenna and the fabricated prototype (AUT) is used as receiving antenna in the anechoic chamber. The AUT was rotated by 360° in both azimuth (horizontal) and elevation (vertical) plane. The radiation patterns are measured using fully automated measurement system at different frequencies of the antenna.

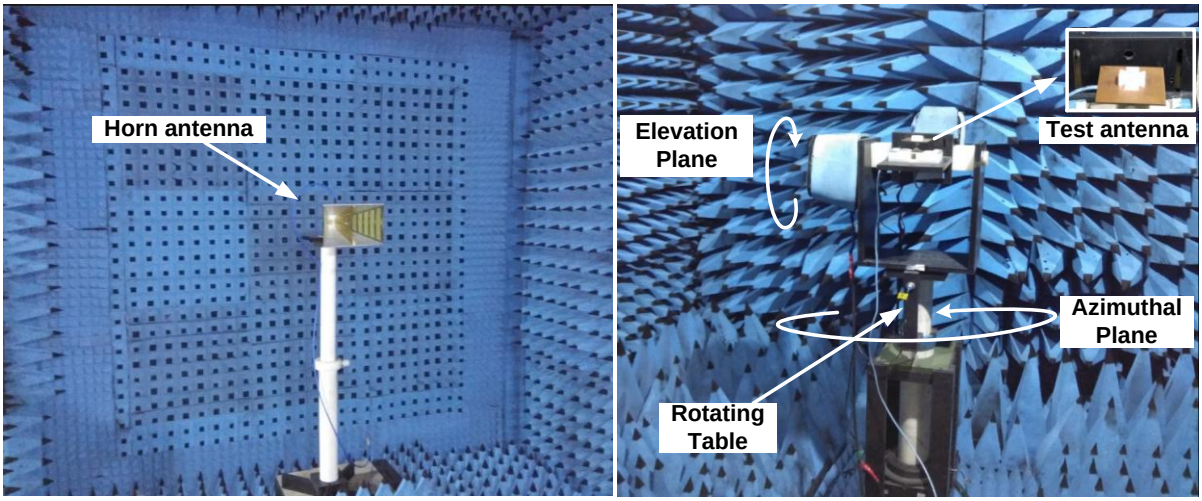

Figure 6.3 Antenna measurement setup in the anechoic chamber (a) Reference horn antenna and (b) Test antenna.

6.4 Results and discussion

6.4.1 Parametric study: Reflection coefficient – frequency characteristics

The effects of design parameters, such as probe height, dimensions and dielectric constant of both sections of each triangular antenna element on the –10 dB reflection coefficient bandwidth have been studied. The loss tangent of Teflon and LMAP sections were kept constant at 0.0010 and 0.0006 respectively in this study. The dimensions of both sections

in each triangular element of the TDRA i.e. teflon and LMAP are varied, keeping the total volume of the 4–CTDRA constant to optimize the results through simulation using Ansys HFSS software. Figure 6.4(a) shows the variations of reflection coefficient of the antenna versus frequency by taking antenna geometrical parameters '*a*' and '*b*' as variable parameters keeping antenna dimension '*c*' fixed at 11.258 mm and assuming values of dielectric constant of teflon and LMAP equal to 2.1 (ε_{r1}) and 6.2 (ε_{r2}), respectively. The values of resonating frequency and bandwidth of the antenna were extracted from Figure 6.4(a) and the results are given in Table 6.2 (Observation 1). For the antenna optimized dimensions (a = 3.464 mm, b = 7.794 mm and c = 11.258 mm) and by choosing values of dielectric constant of the two antenna sections as ε_{r1} = 2.1 and ε_{r2} = 6.2, the effect of variation in probe height on the reflection coefficient frequency characteristic of the TDRA was studied through simulation (Figure 6.4(b)) and the results are described in Table 6.2 (Observation 2). The optimized probe height above the ground plane of 5.7 mm was used for the next observation, since maximum bandwidth is achieved at this height. For the next observation, the optimized parameters from observations 1 and 2 were taken into account i.e. probe height = 5.7 mm, a = 3.464 mm, b = 7.794 mm and c = 11.258 mm. The dielectric constant values of the two sections of each triangular element were varied to observe –10 dB reflection coefficient bandwidth (Figure 6.5) and gain performance of corresponding antennas (given in Table 6.3). From Table 6.3, it is found that maximum impedance bandwidth of 62.05 % and gain of 4.75 dB are obtained in case of antenna having ε_{r1} = 2.1 and ε_{r2} = 8. But, for the antenna having ε_{r1} = 2.1 and ε_{r2} = 6.2, the obtained bandwidth is nearly 62% (i.e. 61.65%) but the gain value of 5.63 dB is higher by 1dB than the previous case. Therefore, the proposed composite TDRA is chosen with the combination of triangular element sections having ε_{r1} = 2.1 and ε_{r2} = 6.2.

Simulated optimized dimensions: '*a*' = 3.464 mm, '*b*' = 7.746 mm, '*c*' = 11.258 mm, dielectric constant of inner dielectric ε_{r2} = 6.2, dielectric constant of outer dielectric ε_{r1} = 2.1 and probe height above the ground plane *Hp* = 5.7mm, are obtained to achieve the wide impedance bandwidth of 61.65 % with resonant frequency of 9.3 GHz and highest gain of 5.63 dB. It is to be noted that loss tangent values of inner dielectric (LMAP) and outer dielectric (Teflon) were assumed fixed at 0.0006 and 0.0010, respectively. Antenna prototype for the proposed design was fabricated and its performance was investigated experimentally. The –10 dB reflection coefficient bandwidth of 7.70 – 15.30 GHz (66.09%) was obtained for the fabricated prototype with the resonant frequency (f_r) of 9.10 GHz (Figure 6.6). It can be inferred from the present study that simulated and measured resonant frequencies and bandwidths of the proposed antenna are nearly in agreement with each other. The deviation in the values of simulated and measured resonant frequency and bandwidth may have been caused due to fabrication and measurement errors including the effect of thin adhesive layer used to make a bond between the ceramic material and teflon.

Table 6.2 Antenna parameters optimized from simulation studies.

Observation 1					**Observation 2**			
ε_{r1} =2.1 , ε_{r2} = 6.2 , *c* = 11.258 mm, H_p = 5.7 mm					ε_{r1} = 2.1, ε_{r2} = 6.2, *a* = 3.464 mm, *b* = 7.794 mm, *c* = 11.258 mm			
***a* (mm)**	***b* (mm)**	**f_r**	**Bandwidth, GHz**	**BW %**	**H_p (mm)**	**f_r**	**Bandwidth, GHz**	**BW %**
1.732	9.526	9.41	8.26 – 11.2	30.22	4.7	11.42,14.74	9.45 – 15.88	50.77
3.464	7.794	9.30	7.82 – 14.79	61.65	5.2	10.75	8.36 – 15.70	61.01
5.196	6.062	9.84	7.82 – 12.85	48.67	5.7	9.3	7.82 – 14.79	61.65
6.928	4.330	9.40	8.11 – 11.25	32.44	6.2	8.54	7.41 – 11.29	41.50
8.660	2.598	8.85	7.95 – 10.38	26.51	6.7	7.94	6.91 – 10.37	38.70

BW: Bandwidth; f_r : Resonant frequency; H_p: probe height

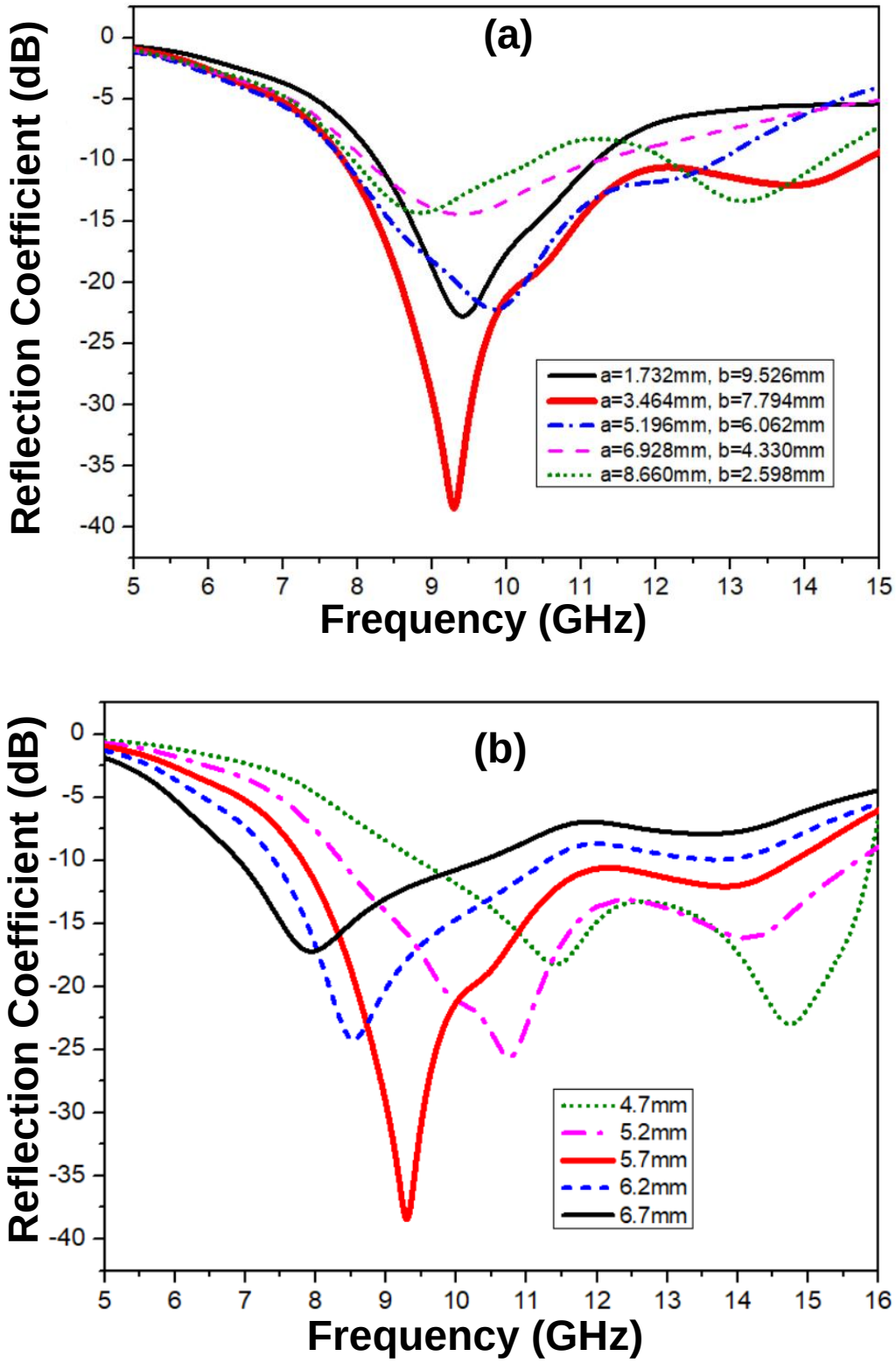

Figure 6.4 Variations of simulated reflection coefficient of 4–CTDRA versus frequency (a) for different values of antenna dimensions '*a*' and '*b*' keeping its dimension '*c*' fixed at 11.258 mm and (b) for different probe heights (assuming *a* = 3.464 mm, *b* = 7.794 mm and *c* = 11.258 mm).

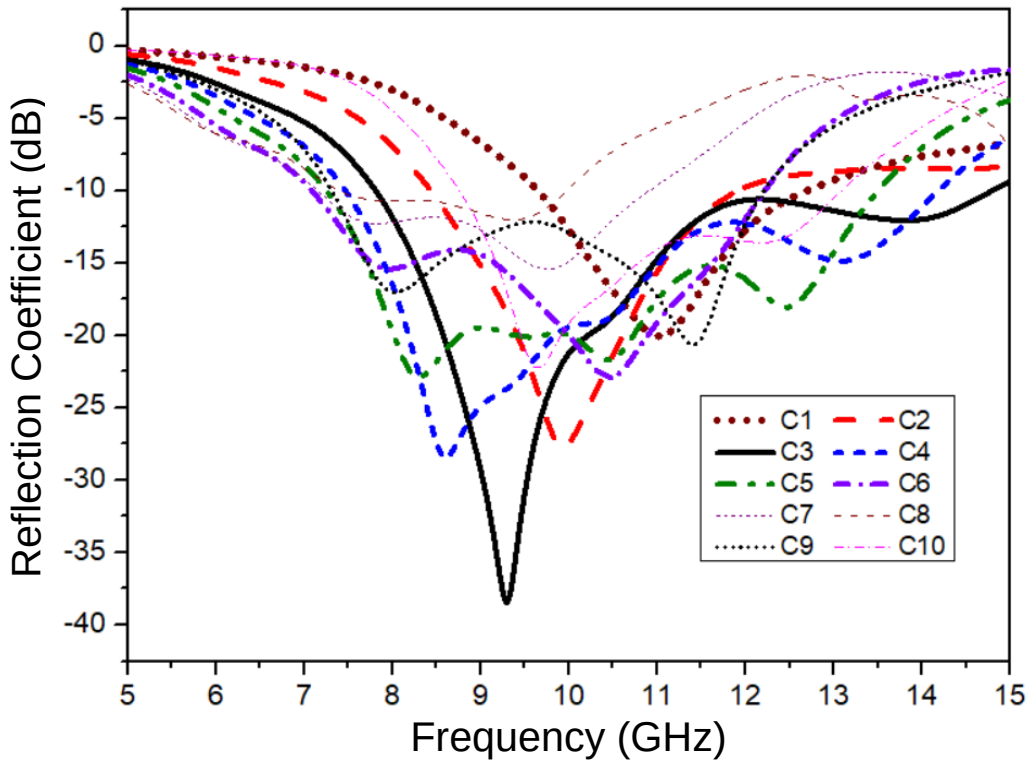

Figure 6.5 Variations of simulated reflection coefficient of 4–CTDRA versus frequency for different dielectric combinations *C1 – C10* (as illustrated in Table III).

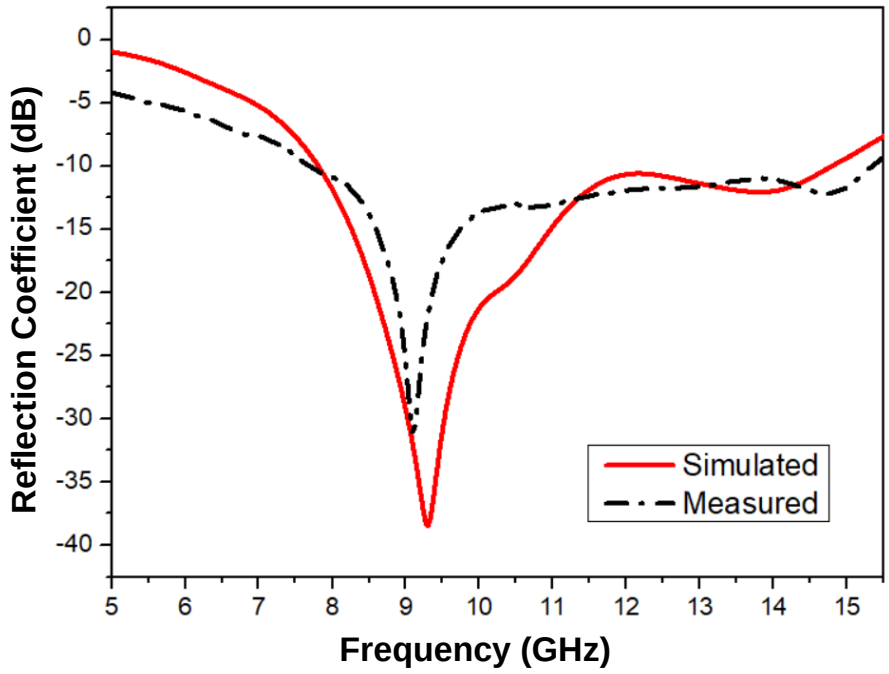

Figure 6.6 Variations of simulated and measured values of reflection coefficient of the proposed antenna vs. frequency.

Table 6.3 Observation 3 – Antenna parameters optimized from simulation study [a = 3.464 mm, b = 7.794 mm, c = 11.258 mm and H_p = 5.7 mm, loss tangent of Teflon = 0.0010, loss tangent of LMAP = 0.0006]

Combinations	ε_{r1}	ε_{r2}	f_r	BW (GHz)	BW (%)	Gain (dB)
C1	2.1	2.1	11.03	9.65 – 12.69	27.21	5.21
C2	2.1	4	9.93	8.43 – 11.90	34.13	4.67
C3	**2.1**	**6.2**	**9.30**	**7.82 – 14.79**	**61.65**	**5.63**
C4	2.1	8	8.60	7.57 – 14.38	62.05	4.41
C5	2.1	10	-	7.25 – 13.50	60.24	4.11
C6	2.1	15	7.97,10.46	7.10 – 12.23	53.078	5.77
C7	2.1	20	9.76	7.15 – 10.91	41.63	5.26
C8	2.1	25	9.37	7.39 – 9.97	29.72	5.74
C9	6.2	6.2	8.03,11.41	7.32 – 12.21	50.07	5.20, 4.81
C10	6.2	2.1	9.65	8.76 – 13.09	39.45	5.50

ε_{r1}: Dielectric constant of outer dielectric; ε_{r2}: Dielectric constant of inner dielectric with triangular cross-section; f_r: Resonant frequency; BW: Bandwidth.

6.4.2 Near field distributions

The simulation study of the near field distribution of the proposed TDRA was carried out at resonant frequency of 9.30 GHz using the Ansoft HFSS numerical simulation software. The electric and magnetic field distributions of the proposed TDRA at different frequencies are shown in Figure 6.7 (a – e). The electric and magnetic fields generated in small ceramic (inner section) of each element of the proposed 4–CTDRA spread in the surrounding outer rhombohedral section made of Teflon. Thus, the field distributions in the proposed 4–CTDRA show that the generated mode in the proposed antenna is TM^z_{101} mode occurring at its resonating frequency of 9.30 GHz. TM^z mode represents that there is no magnetic field component in the z direction. The field distribution get distorted at higher frequency end of the operating bandwidth of antenna (Figure 6.7 (e) and (f)). This may be due to generation of higher order modes.

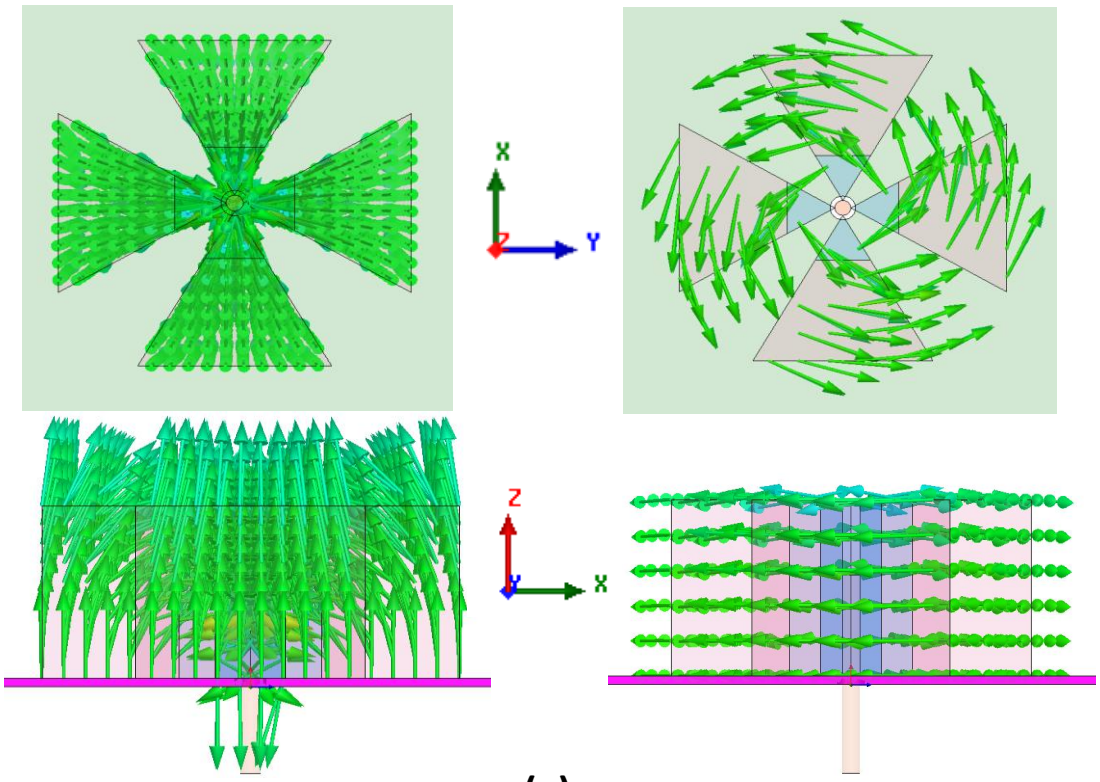

Figure 6.7 Near field distribution of the proposed CTDRA at (a) 7.82 GHz (b) 9.30 GHz in different planes [Left and right side represents E – Field and H – field, respectively].

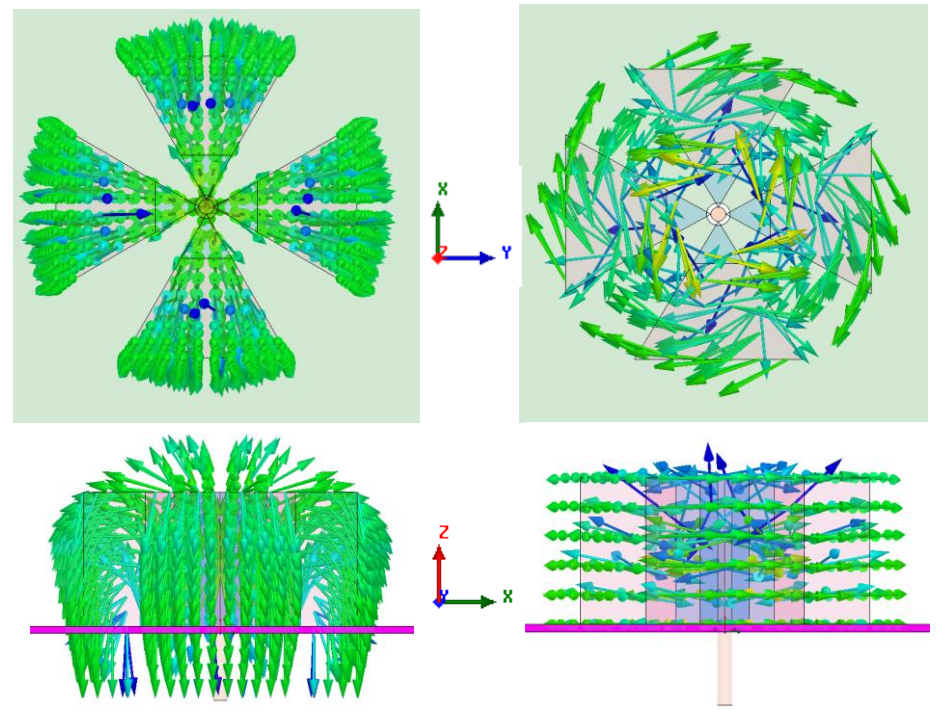

(c)

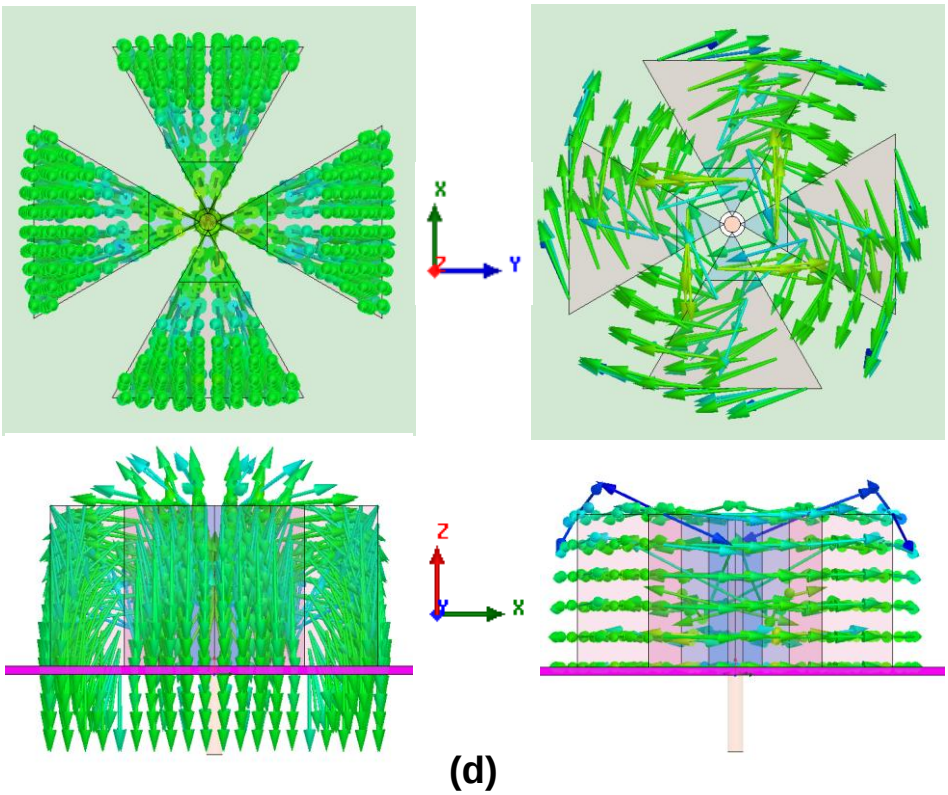

(d)

Figure 6.7(contd.) Near field distribution of the proposed CTDRA at (c) 12.00 GHz (d) 13.50 GHz in different planes [Left and right side represents E – Field and H – field, respectively].

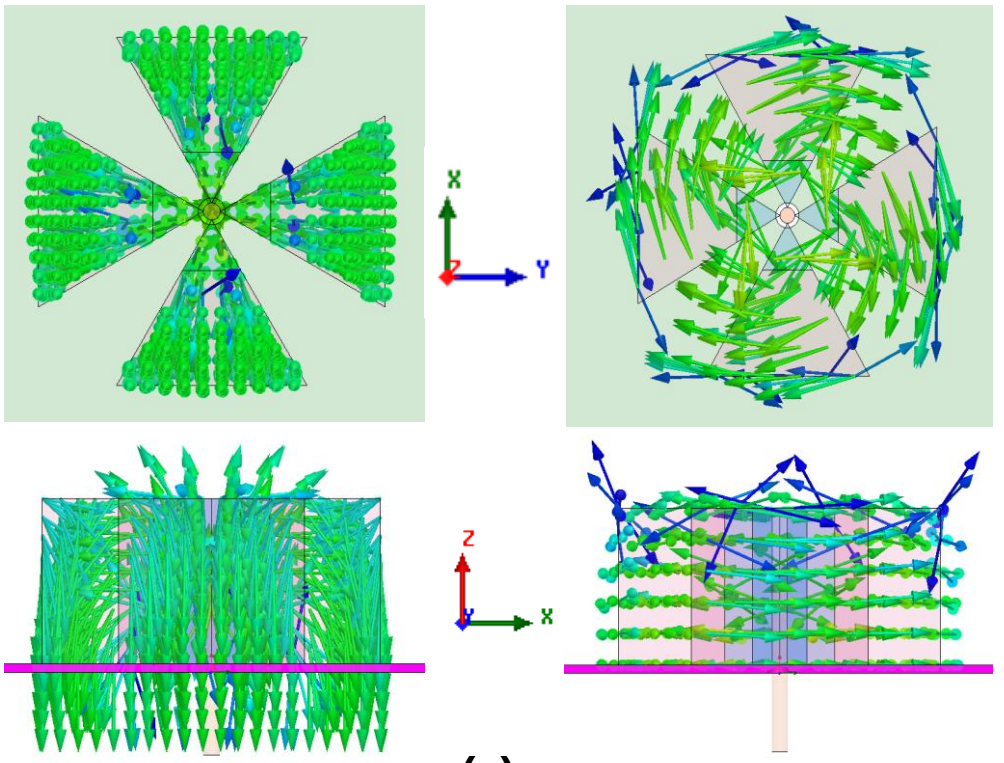

Figure 6.7 (contd.) Near field distribution of the proposed CTDRA at (e) 14.00 GHz and (f) 14.79 GHz in different planes [Left and right side represents E – Field and H – field, respectively].

6.4.3 Radiation patterns and gain

The far field patterns of the proposed antenna at different frequencies over the operating bandwidth were studied through simulation (using Ansoft HFSS software) as well as experiment. The simulated and measured radiation patterns of the proposed antenna in x – z and y – z planes are shown in Figure 6.8. It shows that simulated and experimental radiation patterns are nearly in agreement with each other. No radiation in the broadside direction is observed. This is because the electric field components face their counter vectors. The elements of the proposed antenna structure effectively produces identical radiation fields at the resonant frequency of 9.30 GHz. The proposed antenna shows monopole like radiation patterns at different frequencies due to symmetric arrangement of 4 – composite triangular elements across the probe.

The monopole like radiation patterns are uniform and consistently symmetric over the frequency range 7.82 – 14 GHz. The patterns get distorted at higher end of operating frequency band of the proposed antenna i.e. in the frequency range 14 – 14.79 GHz which may be due to the generation of higher order modes.

Figure 6.9 (a – d) shows simulated 3D gain plot of proposed 4 element CTDRA at different frequencies. We observed that since the DRA elements are put in the azimuthal plane, high gain is obtained in this plane. Null around z– direction is broadened at higher frequencies (Figure 6.9 (d)). 3D gain plot shown in Figure 6.9 indicates uniform radiation through the DRA. The proposed DRA shows that it can be used as omnidirectional antenna. The variations of simulated and measured gain values of the proposed antenna versus frequency over operating bandwidth are shown in Figure 6.10. The results for the simulated and measured gain values of the proposed antenna are nearly in agreement with each other. Gain values of the proposed antenna are oscillatory in nature over its

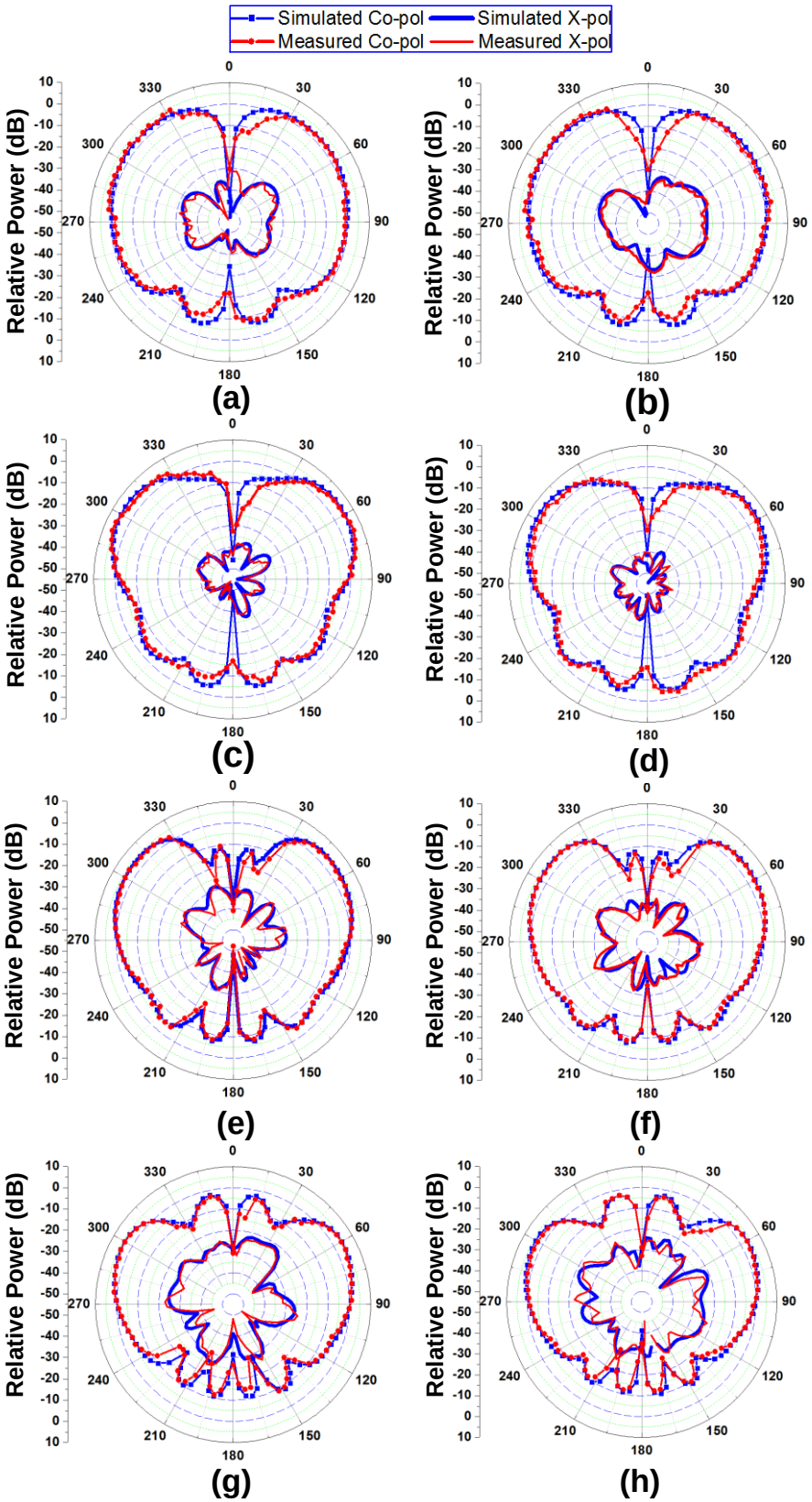

Figure 6.8 Radiation pattern of proposed 4–CTDRA at (a) 7.82 GHz [x-z plane], (b) 7.82 GHz [y-z plane], (c) 9.30 GHz [in x-z plane], (d) 9.30 GHz [y-z plane], (e) 12.00 GHz [x-z plane], (f) 12.00 GHz [y-z plane], (g) 14.79 GHz [x-z plane] and (h) 14.79 GHz [y-z plane].

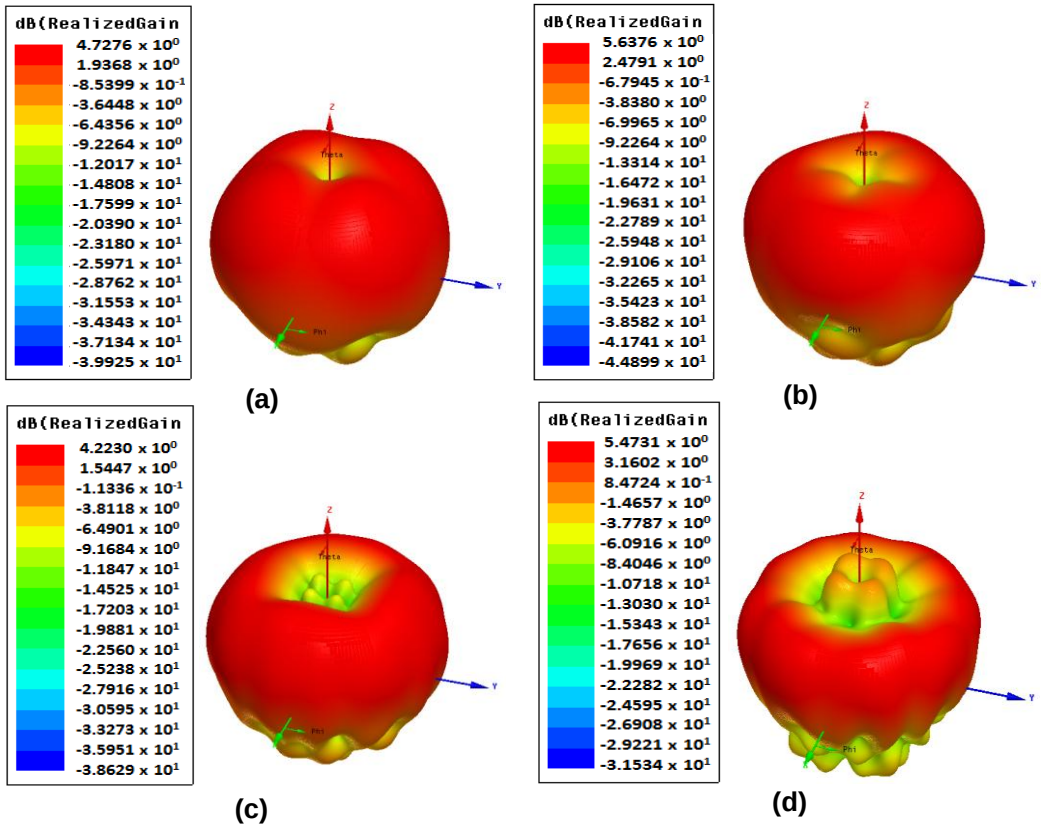

Figure 6.9 3D gain plot of proposed 4–CTDRA at (a) 7.82 GHz, (b) 9.30 GHz, (c) 12.00 GHz, and (d) 14.79 GHz.

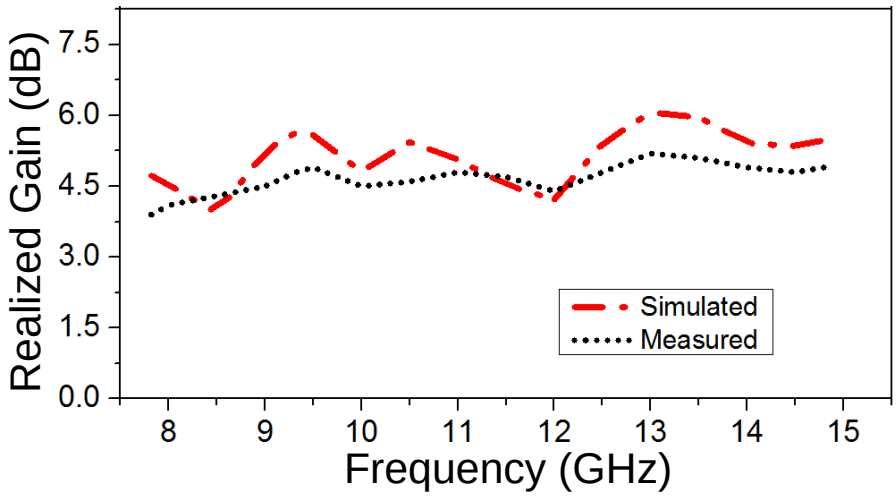

Figure 6.10 Variations of measured and simulated gain values of the proposed 4–CTDRA versus frequency.

operating frequency band. This is because signal is experiencing different phase delays at different frequencies while traversing the two dielectric sections of the proposed antenna. From the gain plots it is figured out that the simulated realized gain values lie in the range 3.923 – 6.065 dB over its operating frequency band, with an average gain value of 5.142 dB. The measured gain values are found to lie in the range 3.90 – 5.20 dB over the operating frequency range of the proposed antenna, with average gain values of 4.658 dB.

6.4.4 Comparison with other antennas available in literature

Some of the investigations has been made on different multi element DRAs for the generation of monopole like radiation pattern. The design and performance of the proposed TDRA is compared with the other antennas reported in literatures and given in Table 6.4.

Table 6.4 Comparison of the proposed antenna results with the antenna reported in literatures for monopole like radiation pattern

Parameters	**Guha et al. (2006)**	**Gangwar et al. (2017)**	**Chaudhary et al. (2012)**	**Proposed TDRA**
Excitation	Modified coaxial probe (coaxial probe surrounded by small dielectric rod)	Coaxial Probe	Modified coaxial probe (coaxial probe surrounded by multilayer multi-permittivity (MLMP) dielectric layers)	Coaxial Probe
Resonators	4–element Cylindrical resonator	4–element triangular resonator	3–element MLMP cylindrical resonator	4–element composite triangular resonator
Operating Frequency Range	~3 – 4 GHz	4.7 – 6.8 GHz	3.9 – 6.2 GHz	7.7 – 15.3 GHz
Bandwidth %	~29 %	~37 %	~53 %	~66 %
Gain	4dB	4.76	5.7 dB	4.6dB
Fabrication	Complex	Easy	Very complex	**Easy**

The detail investigations of the three reference papers which are listed in Table 6.4 is described in detail with diagrams showing their results in Chapter 1 (section 1.1.6). Out of these three, bandwidth of 52.90 % with gain of 5.7 dB is obtained by **Chaudhary et al. (2012)**. But its fabrication is very complex, as it uses multi layer multi permittivity modified coaxial probe along with the 3-element multi layer multi permittivity cylindrical resonators. So, in the proposed design of TDRA, maximum bandwidth of 66.09% is achieved with reasonable good gain of 4.6 dB.

6.5 Summary

The proposed four element CTDRA consists of two different dielectric materials for each element. Inner dielectric of each antenna element touching the coaxial probe is made of LMAP (ε_r = 6.2 and tanδ = 0.0006) while outer dielectric is made of teflon (ε_r = 2.1 and tanδ = 0.0010). The proposed antenna has provided simulated -10 dB reflection coefficient bandwidth of 6.97 GHz (61.65 %) with an average gain of 5.142 dB over its operating frequency range 7.82 – 14.79 GHz. The experimental -10 dB reflection coefficient bandwidth of 7.6 GHz (66.09 %) with average gain of 4.658 dB has been obtained over the operating frequency range of the proposed antenna. Monopole like radiation patterns have been obtained over the operating frequency band of the proposed antenna though little distortion has been observed at higher frequencies due to generation of higher order modes. The proposed antenna can potentially be used in broadcast base-station, radar and satellite communication and will provide wide area coverage.